

Cite this: *Mater. Adv.*, 2021, 2, 2600Received 18th January 2021,  
Accepted 12th March 2021

DOI: 10.1039/d1ma00041a

rsc.li/materials-advances

## Enhanced linear thermosensitivity of gel-immobilized colloidal photonic crystal film bound on glass substrate†

Toshimitsu Kanai, \* Naoto Kobayashi and Hiroyuki Tajima

**In this study, colloidal crystals were immobilized in a linear thermosensitive copolymer hydrogel film that was simultaneously bound on a glass substrate using a silane coupling agent via photopolymerization. Due to the suppression of the in-plane shrinkage of the gel, the thermosensitivity increased 1.6-fold, while the linear sensitivity was maintained.**

Gel-immobilized colloidal photonic crystals are three-dimensional periodic arrays of monodisperse colloidal particles, which are embedded in soft polymer gels.<sup>1–5</sup> They have optical stop bands and exhibit a bright reflection colour due to the Bragg reflection at the optical stop-band wavelength in the visible light region.<sup>6,7</sup> These gels have a unique characteristic that their volume changes in response to an external stimulus. Therefore, the reflection colour or optical stop-band wavelength can be tuned by changing the lattice constant by external stimulus. Consequently, they are expected to find applications in tunable lasers, tunable optical filters, chemical and biological sensors for detecting change through the Bragg wavelength, *etc.*<sup>8–12</sup> So far, tunable colloidal photonic crystals responding to various external stimuli (*e.g.*, change in temperature, pH, and solvent) have been reported.<sup>13,14</sup> For practical applications, high and linear sensitivity in a wide range of stimulus intensities is beneficial. However, in general, the volume change in gel is a type of phase transition.<sup>15–18</sup> For example, poly(*N*-isopropylacrylamide) (PNIPAM) is a typical thermosensitive polymer that exhibits a volume phase transition at 32 °C.<sup>19–21</sup> Thus, the Bragg wavelength of the colloidal crystals immobilized in PNIPAM gel changes significantly at the transition temperature and does not change above that temperature. Although thermosensitivity can be adjusted by varying the concentration of monomers and cross-linkers in the gel,<sup>22</sup> obtaining high and linear sensitivity over a wide temperature range is still a challenging task. We previously reported the Bragg wavelength

of colloidal crystals immobilized in copolymer hydrogels consisting of thermosensitive *N*-isopropylacrylamide (NIPAM) and non-thermosensitive *N*-methylolacrylamide (NMAM) monomers; the Bragg wavelength of these crystals showed linear thermosensitivity over a wide temperature range, although the sensitivity was small (−0.39 to −2.1 nm °C<sup>−1</sup>).<sup>23</sup> Moreover, we recently discovered a promising approach for enhancing the thermosensitivity of a disc-shaped PNIPAM-immobilized colloidal crystal film by pinching the circular edge with washers.<sup>24</sup> This pinch restrained the in-plane shrinkage of the gel, which led to an enhanced contraction of the lattice spacing in the thickness direction; further, the Bragg wavelength could be controlled with a high thermosensitivity over a wide wavelength range.

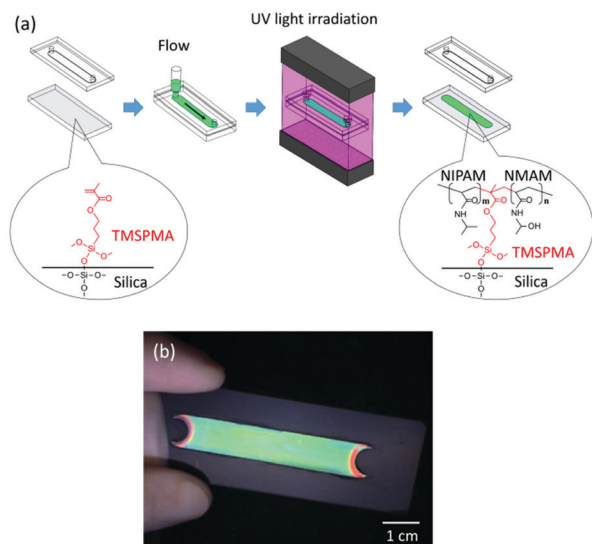
In this study, we demonstrate that the linear thermosensitivity of colloidal crystals immobilized in a copolymer hydrogel film composed of PNIPAM and poly(*N*-methylolacrylamide) (PNMAM) can be enhanced. This is achieved while maintaining linear sensitivity by chemically binding the film on a glass substrate using a silane coupling agent; this provides easier sample preparation, handling, and scaling up than the pinching method. We show that the film chemically bound on the substrate exhibits a uniform Bragg reflection colour change from red to blue without any change in the film area and without the generation of wrinkles upon heating. Owing to the suppression of the in-plane shrinkage, the thermosensitivity increases 1.6-fold, while linear sensitivity is maintained in the temperature range from 10 °C to 50 °C. We also show that the film exhibits excellent reversibility and repeatability of the change in the Bragg wavelength.

Fig. 1a shows the overall process for the preparation of the gel-immobilized colloidal photonic crystal film bound on a glass substrate (see the ESI,† for details). An aqueous suspension of uniform-sized polystyrene particles with a diameter of 140 nm was deionized using a mixed-bed ion-exchange resin to form a crystal phase. The colloidal crystal was mixed with the gelation reagent containing NIPAM and NMAM monomers, an *N,N'*-methylenebisacrylamide (BIS) cross-linker, and a 2,2'-azobis[2-methyl-*N*-(2-hydroxyethyl)propionamide] (VA) photoinitiator.

Yokohama National University, 79-5 Tokiwadai, Hodogaya, Yokohama, Kanagawa 240-8501, Japan. E-mail: tkanai@ynu.ac.jp

† Electronic supplementary information (ESI) available: Experimental procedure and supporting figure. See DOI: 10.1039/d1ma00041a





**Fig. 1** (a) Schematic representation of preparation process for gel-immobilized colloidal photonic crystal film bound on glass substrate. (b) Photograph of obtained gel-immobilized colloidal photonic crystal film bound on glass substrate.

The surface of a slide glass was modified with a silane coupling agent, 3-(trimethoxysilyl)propyl methacrylate (TMSPMA),<sup>25,26</sup> and used as a bottom substrate of a flat capillary cell. The colloidal crystal containing the gelation reagent (particle concentration: 11.3 vol%; NIPAM: 440 mM; NMAM: 360 mM; BIS: 40 mM; VA: 0.5 mM) was shear-flowed into a flat capillary cell (flow channel thickness: 0.1 mm; width: 9 mm; and length: 50 mm) to convert the colloidal crystal structure into a single crystal in the whole cell.<sup>27,28</sup> The NIPAM, NMAM, BIS, and TMSPMA were polymerized by uniform ultraviolet (UV) light irradiation from both sides of the cell surface at 25 °C for 2 h.<sup>23,29</sup> The polymer network composed of NIPAM, NMAM, and BIS immobilized the colloidal crystals and simultaneously connected to the inorganic siloxane network of the glass substrate through covalent bonding with the TMSPMA. After removing the top substrate, the colloidal crystal gel film bound on the bottom substrate was obtained. The film exhibited a uniform reflection colour for a large area (Fig. 1b). The flat capillary cell with the bottom substrate uncoated with the TMSPMA was used to prepare the gel-immobilized colloidal crystal film that was unbound on the substrate. Both films (bound and unbound on the substrates) were placed in a water bath. The temperature of water was increased from 10 °C to 50 °C, and photographs and reflection spectra of the films at normal incidence were recorded at various temperatures.

Upon increasing the temperature from 10 °C to 50 °C, the gel-immobilized colloidal crystal film unbound on the substrate shrank; this resulted in the reflection colour changing from orange to yellow and then to green (Fig. 2a). However, the large-area film formed wrinkles during the shrinkage. In the reflection spectra, a large width of reflection peak was observed because of the wrinkles. The peak was due to the Bragg reflection derived from the face-centered cubic (FCC) (111) lattice planes perpendicular to the film surface and shifted to the shorter

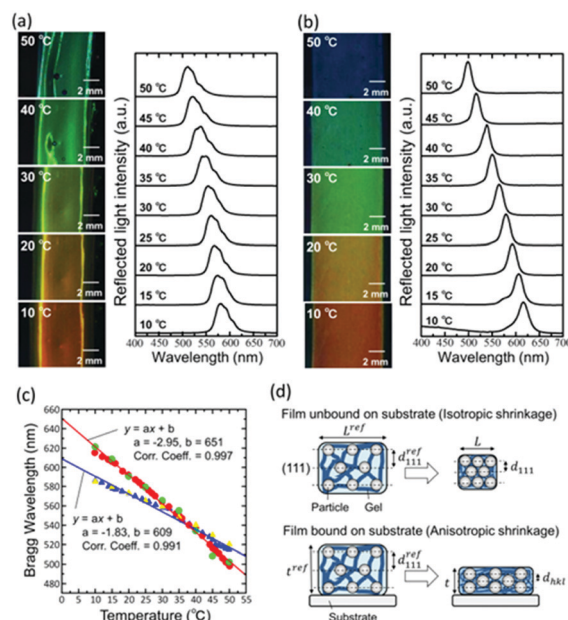


**Fig. 2** Photographs and reflection spectra of gel-immobilized colloidal crystal films (a) unbound and (b) bound on substrates at various temperatures. (c) Bragg wavelengths of gel-immobilized colloidal crystal films as a function of temperature (experimentally measured Bragg wavelength of film unbound on substrate (blue triangle) and bound (red circle) on substrates, Bragg wavelength of film unbound on substrate calculated from change in length in-plane direction (yellow triangle), and Bragg wavelength of film bound on substrate calculated from change in film thickness (green circle)). (d) Schematic representation of lattice spacing of colloidal crystals immobilized in gel films unbound and bound on substrates.

wavelength linearly with the increase in temperature. In contrast, the gel-immobilized colloidal crystal film bound on the substrate did not wrinkle during heating (Fig. 2b). Furthermore, the in-plane area of the film was not reduced owing to the suppression of the in-plane shrinkage of the gel due to binding on the substrate. As a result, the film exhibited a larger span of wavelengths (*i.e.*, from red to blue reflection colours), while maintaining uniformity for a large area when the temperature was increased from 10 °C to 50 °C. In the spectra, the reflection peak shift was greater than that of the unbound film. The plots in Fig. 2c show the Bragg wavelengths of the gel films unbound and bound on the substrates as a function of temperature, which were determined from Fig. 2a and b, respectively. The film unbound on the substrate exhibited linear thermosensitivity with a slope of  $-1.83 \text{ nm } ^\circ\text{C}^{-1}$ . Conversely, the film bound on the substrate exhibited an enhanced linear thermosensitivity of  $-2.95 \text{ nm } ^\circ\text{C}^{-1}$ , which corresponded to about a 1.6-fold increase as compared to that of the unbound film. Thus, we found that binding the film on the substrate provided significant benefits for practical utilization, such as easier sample preparation and handling, suppression of the generation of wrinkles, a constant film area, and enhanced thermosensitivity.

The enhanced thermosensitivity is quantitatively explained using Bragg's Law for normal incidence as follows:

$$\lambda_{hkl} = 2n_c d_{hkl} \quad (1)$$



where  $\lambda_{hkl}$  is the Bragg wavelength,  $n_c$  is the refractive index of the colloidal crystals, and  $d_{hkl}$  is the lattice spacing of ( $hkl$ ) planes perpendicular to the incident light. The value of  $n_c$  can be approximated by the volume-weighted average of the refractive indices of the components,<sup>24,30</sup>

$$n_c = n_p \phi_p + n_{\text{gel}} \phi_{\text{gel}} \quad (2)$$

where  $n_p$  ( $n_p = 1.59$ ) and  $\phi_p$  are the refractive index and volume fraction of polystyrene particles, respectively, and  $n_{\text{gel}}$  and  $\phi_{\text{gel}}$  are the refractive index and volume fraction of the hydrogel, respectively. Because the hydrogel consists of the polymer and water,  $n_{\text{gel}}$  can be approximated as  $n_{\text{gel}} = n_{\text{pol}} \phi_{\text{pol}} / \phi_{\text{gel}} + n_w \phi_w / \phi_{\text{gel}}$ , where  $n_{\text{pol}}$  ( $n_{\text{pol}} = 1.43$ ) and  $n_w$  ( $n_w = 1.33$ ) are the refractive indices of the polymer and water, respectively, and  $\phi_{\text{pol}}$  and  $\phi_w$  are the volume fractions of the polymer and water in the gel-immobilized colloidal crystal film, respectively. The relation between  $\phi_{\text{pol}}$  and  $\phi_p$  is given from the amounts of the polystyrene particles and gelation reagent added as  $\phi_{\text{pol}} = 0.80 \phi_p$ .

For the film unbound on the substrate, the gel shrinks isotropically in three dimensions; further, the colloidal crystals embedded in the gel retain the FCC structure with the (111) lattice planes normal to the thickness direction during shrinkage (Fig. 2d). Thus, the lattice spacing perpendicular to the incident light at any temperature is  $d_{111}$ ; this is determined from the reference (111) lattice spacing  $d_{111}^{\text{ref}}$ , which represents the (111) lattice spacing at 25 °C. Reference length  $L^{\text{ref}}$  represents a length in-plane direction of the film at 25 °C, and the length in-plane direction  $L$  at any temperature. Therefore,  $d_{111}$  is calculated as follows:

$$d_{111} = \frac{L}{L^{\text{ref}}} d_{111}^{\text{ref}} \quad (3)$$

In addition, the particle volume fraction  $\phi_p$  for the FCC structure is given using  $d_{111}$  and particle diameter  $d$  as follows:

$$\phi_p = \frac{2\pi}{9\sqrt{3}} \left( \frac{d}{d_{111}} \right)^3 \quad (4)$$

The  $d_{111}^{\text{ref}}$  is calculated by substituting the observed Bragg wavelength at 25 °C into eqn (1) and then using eqn (2) and (4). By substituting the measured  $L^{\text{ref}}$  and  $L$  into eqn (3) and using eqn (1), (2), and (4), the Bragg wavelength is estimated; further, it is plotted as the open triangle in Fig. 2c. These plots are in reasonable agreement with the plots of the observed Bragg wavelength.

In contrast, the colloidal crystals immobilized in the gel film that is bound on the substrate do not retain the FCC structure during shrinkage owing to the suppression of the in-plane shrinkage of the gel (Fig. 2d). In this case, the lattice spacing normal to the incident light  $d_{hkl}$  at any temperature is given as follows by using the reference (111) lattice spacing  $d_{111}^{\text{ref}}$ , reference film thickness  $t^{\text{ref}}$  (film thickness at 25 °C), and film thickness  $t$  at any temperature:

$$d_{hkl} = \frac{t}{t^{\text{ref}}} d_{111}^{\text{ref}} \quad (5)$$

In addition, the particle volume fraction  $\phi_p$  is found by using the reference particle volume fraction  $\phi_p^{\text{ref}}$  (particle volume fraction at 25 °C),  $t^{\text{ref}}$ , and  $t$ :

$$\phi_p = \frac{t^{\text{ref}}}{t} \phi_p^{\text{ref}} \quad (6)$$

The  $d_{111}^{\text{ref}}$  and  $\phi_p^{\text{ref}}$  are calculated by substituting the measured Bragg wavelength of the film bound on the substrate at 25 °C into eqn (1) and then using eqn (2) and (4). By substituting the measured  $t^{\text{ref}}$  and  $t$  (ESI,† Fig. S1) into eqn (5) and (6) and using eqn (1) and (2), the Bragg wavelength is calculated and plotted as the open circle in Fig. 2c. These plots are in good agreement with the plots of the observed Bragg wavelength of the film bound on the substrate. The validity of eqn (2) and uniformity of the thermal compressibility of the gel film are attributed to the correspondence.

The film bound on the substrate showed excellent reversibility and repeatability of the reflection colour change. When the film with yellowish colour at 20 °C was put into a water bath at 10 °C, the colour changed to red (Fig. 3a). The Bragg peak showed a redshift, and the wavelength reached a constant value of  $617 \pm 1$  nm in 4 min. When the film was subsequently put into a water bath at 40 °C, the peak showed a blue shift; this resulted in the colour changing to green. When the film was put back into a water

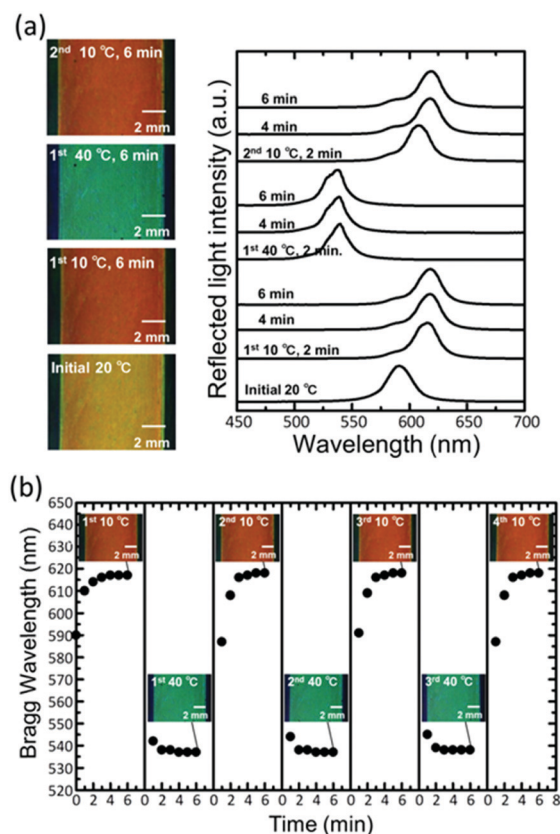


Fig. 3 (a) Photographs and reflection spectra of gel-immobilized colloidal crystal film bound on substrate after temperature change. (b) Plots of Bragg wavelength and photographs of film by repeating temperature change between 10 °C and 40 °C for three cycles.



bath at 10 °C, the colour changed to red again. Further, the Bragg peak returned to the same wavelength. Fig. 3b shows the plots of the Bragg wavelength and photographs of the film by repeating the temperature change between 10 °C and 40 °C for three cycles. The Bragg wavelength returned to the same value at the same temperature. The variation in the Bragg wavelength did not exceed a few percent after 10 cycles, and no damage was observed to the film.

In summary, we have demonstrated that the linear thermo-sensitivity of colloidal crystals immobilized in a copolymer hydrogel film composed of PNIPAM and PNMAM could be enhanced by chemically binding them on a glass substrate using a silane coupling agent. The large-area film exhibited a uniform Bragg reflection colour change from red to blue without the generation of wrinkles when the temperature was increased from 10 °C to 50 °C. Due to the suppression of the in-plane shrinkage of the gel, the film area did not reduce and the thermosensitivity increased 1.6-fold; this was achieved while maintaining linear sensitivity. The film also exhibited excellent reversibility and repeatability of the change in the Bragg wavelength. Because the present method uses an interfacial phenomenon that binds to the glass substrate to control bulk distortion, a critical film thickness, above which the method fails, will exist. Although we demonstrated the responsiveness of the colloidal crystals toward temperature changes, the principle should also be applicable to gel-immobilized colloidal crystals that respond to other stimuli. The present method contributes significantly to the advancement of the practical applications of gel-immobilized colloidal crystals. Enhanced sensitivity without a change in area is beneficial for utilizing tunable photonic crystals and chemical and biological sensors for monitoring environmental changes through the Bragg wavelength.

## Conflicts of interest

There are no conflicts of interest to declare.

## Acknowledgements

This work was supported by JSPS KAKENHI (Grant Number 25289237). The authors acknowledge Dr Tsutomu Sawada (NIMS) for helpful discussions.

## Notes and references

- J. M. Weissman, H. B. Sunkara, A. S. Tse and S. A. Asher, *Science*, 1996, **274**, 959.
- K. P. Velikov, C. G. Christova, R. P. A. Dullens and A. van Blaaderen, *Science*, 2002, **296**, 106.
- J. Yamanaka, M. Murai, Y. Iwayama, M. Yonese, K. Ito and T. Sawada, *J. Am. Chem. Soc.*, 2004, **126**, 7156.
- T. Kanai, T. Sawada and J. Yamanaka, *J. Ceram. Soc. Jpn.*, 2010, **118**, 370.
- T. Kanai, D. Lee, H. C. Shum and D. A. Weitz, *Small*, 2010, **6**, 807.
- P. Pieranski, *Contemp. Phys.*, 1983, **24**, 25.
- A. K. Arora and B. V. R. Tata, *Ordering and Phase Transitions in Charged Colloids*, VCH, New York, 1996.
- J. Holtz and S. A. Asher, *Nature*, 1997, **389**, 829.
- S. H. Foulger, P. Jiang, A. Lattam, D. W. Smith, J. J. Ballato, D. E. Dausch, S. Grego and B. R. Stoner, *Adv. Mater.*, 2003, **15**, 685.
- H. Fudouzi and Y. Xia, *Adv. Mater.*, 2003, **15**, 892.
- Y. Iwayama, J. Yamanaka, Y. Takiguchi, M. Takasaka, K. Ito, T. Shinohara, T. Sawada and M. Yonese, *Langmuir*, 2003, **19**, 977.
- S. Furumi, T. Kanai and T. Sawada, *Adv. Mater.*, 2011, **23**, 3815.
- J. Wang and Y. Han, *J. Colloid Interface Sci.*, 2011, **353**, 498.
- T. Kanai, D. Lee, H. C. Shum, R. K. Shah and D. A. Weitz, *Adv. Mater.*, 2010, **22**, 4998.
- P. J. Flory, *Principles of Polymer Chemistry*, Cornell University, Ithaca, 1953.
- T. Tanaka, D. Fillmore, S. T. Sun, I. Nishino, G. Swislow and A. Shah, *Phys. Rev. Lett.*, 1980, **45**, 1636.
- S. Katayama, Y. Hirokawa and T. Tanaka, *Macromolecules*, 1984, **17**, 2641.
- A. Toyotama, T. Kanai, T. Sawada, J. Yamanaka, K. Ito and K. Kitamura, *Langmuir*, 2005, **21**, 10268.
- B. R. Saunders and B. Vincent, *Adv. Colloid Interface Sci.*, 1999, **80**, 1.
- R. K. Shah, J. W. Kim, J. J. Agresti, D. A. Weitz and L. Y. Chu, *Soft Matter*, 2008, **12**, 2303.
- T. Kanai, K. Ohtani, M. Fukuyama, T. Katakura and M. Hayakawa, *Polym. J.*, 2011, **43**, 987.
- Y. Takeoka and M. Watanabe, *Langmuir*, 2003, **19**, 9104.
- H. Sugiyama, T. Sawada, H. Yano and T. Kanai, *J. Mater. Chem. C*, 2013, **1**, 6103.
- T. Kanai, H. Yano, N. Kobayashi and T. Sawada, *ACS Macro Lett.*, 2017, **6**, 1196.
- W. J. Huang and W. F. Lee, *Polym. Compos.*, 2010, **31**, 887.
- Z. Osvath, T. Toth and B. Ivan, *Macromol. Rapid Commun.*, 2017, **38**, 1600724.
- T. Sawada, Y. Suzuki, A. Toyotama and N. Iyi, *Jpn. J. Appl. Phys.*, 2001, **40**, L1226.
- T. Kanai, T. Sawada, A. Toyotama and K. Kitamura, *Adv. Funct. Mater.*, 2005, **15**, 25.
- T. Kanai, T. Sawada, A. Toyotama, J. Yamanaka and K. Kitamura, *Langmuir*, 2007, **23**, 3503.
- T. Kanai, S. Yamamoto and T. Sawada, *Macromolecules*, 2011, **44**, 5865.

